

Distribution of oval cells and c-myc mRNA expression in mouse hepatocarcinogenesis

Chi-Hua Fang, Gang-Qing Zhang, Xin-Yong Zhu and Jia-Qing Gong

Guangzhou, China

BACKGROUND: This study was designed to assess the roles of oval cells and c-myc mRNA in the process of hepatocarcinogenesis and to clarify the function of carcinogene c-myc in the development of hepatocellular carcinoma (HCC) and the mechanism of inhibitory function of uscharidin on HCC in mouse hepatocarcinogenesis.

METHODS: A total of 120 clean SD mice were divided into normal group, cancer induction group, and intervention group. The normal group was fed with standard forage while the rest two groups were given p-dimethylaminoazobenzene (DAB) to induce cancer. Thirteen weeks after induction of cancer, the two groups were fed with standard forage and water. Once the pattern was set up, the intervention group was given uscharidin injection into the abdominal cavity from the first week to the 14th week. On the 2nd, 4th, 6th, 8th, 10th, 12th, 14th, 16th, 18th, 20th, 22nd, and 24th week, all mice were killed and biopsied from the liver lobe for pathological analysis. At the same time, the number of tumor nodes was counted and the expression of c-myc mRNA was tested by RT-PCR.

RESULTS: Since the 2nd week after cancer induction, proliferated oval cells could be seen in the portal area. Initially, the oval cells appeared in the cortical layer of the portal area, then proliferated gradually and immigrated into the liver parenchyma. In the period of fibrosis after liver proliferation, proliferated heaps of oval cells were noted in both portal and peripheral areas. In the period of carcinomatous change, oval cells could be seen both outside and inside of cancer nodes, but most of them were distributed outside. The c-myc gene was expressed negatively in the liver tissue of mice. The quantity of the expression began to increase at the time of infection of the liver and tended to increase with the degree of hepatic injury. In the period of canceration, the expression level of c-myc mRNA increased gradually. The intervention of uscharidin could not inhibit but

delay the increase of the expression of c-myc mRNA.

CONCLUSION: Oval cells are closely related to hepatocarcinoma cells, which play an important role in the occurrence and development of hepatocarcinogenesis. Uscharidin can inhibit the occurrence of hepatocarcinogenesis or local spreading at the early stage of cancer induction by DAB, but it cannot inhibit the expression of c-myc.

(*Hepatobiliary Pancreat Dis Int* 2004; 3: 433-439)

KEY WORDS: oval cell; hepatocellular carcinoma; c-myc mRNA; uscharidin

Introduction

At present, liver oval cell is regarded as one of the cell sources of primary hepatocellular carcinoma (HCC).^[1,2] C-myc is a sort of the maintaining gene for malignant tissues. The expression of c-myc is changed when growth factors and hormone irritation signals are transferred from the cell membrane into the cell by N-ras genetic products. The aim of this study was to study how to use 3methyl-2-methyl-azobenzene to evoke HCC in mice, the distribution of oval cells, and the expression level of c-myc mRNA in an attempt to identify the effect of carcinogene on the development of HCC and the inhibitory mechanism of uscharidin on HCC.

Methods

Subjects

One hundred-twenty SD mice of both sexes, weighing 100-120 g provided by the Animal Experimental Center of Zhongshan University, Guangzhou, China, were fed by the Animal Feeding Unit, Zhujiang Hospital of the First Military Medical University. Test kit extracting total RNA, DNA marker (100bp), PCR primer and Rnase were purchased from the Huamei Bioengineering Corp., Guangzhou, China. M-MLV reverse transcriptase was obtained from Promega Corp., USA, Tag DNA polymerase from Gibco Corp., USA, 4 × dNTP from Sigma Corp., USA. RT-PCR amplification primer was synthesized by Shanghai Biotech Corp., Shanghai, China in accordance with the Genebank reference. C-myc primers

Author Affiliations: Department of Hepatobiliary Surgery, Zhujiang Hospital of the First Military Medical University, Guangzhou 510282, China (Fang CH, Zhang GQ, Zhu XY and Gong JQ)

Corresponding Author: Chi-Hua Fang, MD, Department of Hepatobiliary Surgery, Zhujiang Hospital of the First Military Medical University, Guangzhou 510282, China (Tel: 86-20-61642926; Fax: 86-20-61643020; Email: fch58520@sina.com)

This work was supported by two grants from the Science Foundation of Guangdong Province, China (No. 010593; No. 020097).

© 2004, Hepatobiliary Pancreat Dis Int. All rights reserved.

were; sense 5'-TCTTCTTCCCTCGGACTCGCT-3', antisense 5'-GGTGTGTTTTGGAGGTCGT-3' 228bp. β -actin primers were; sense 5'-ACCCCACTGAAA-AAGATGA-3', antisense 5'-ATCTTCAAACCTCC-ATGATG-3' 120bp. Main reagent dispersion, and Tris-acetic acid ethylenediaminetetraacetic acid (TAE) depot buffer solution contained 242 g Tris alkali, 57.1 ml ice vinegar, and 100 ml 0.5 mol/L EDTA (pH 8.0), which were mixed evenly.

Establishment of hepatocarcinoma pattern

With modified methods of cancer induction,^[3,4] p-dimethylaminoazobenzene (DAB) was evenly added into standard forage, with a proportion of 0.06% in the mixture. Each mouse was given 15-20 g/d (about 0.010 g DAB/d) of the mixture, and regular water, and kept at a room temperature of 25-28 °C. From the 14th week of cancer induction, the forage with DAB was replaced with standard forage and water. The normal group of mice was fed with standard forage.

Groups and treatment

The 120 SD mice were divided into normal group (group A, 24 mice), cancer induction group (group B, 48), and intervention group (group C, 48). Each group was further divided into 12 subgroups. Thus one normal subgroup consisted of 2 mice and each subgroup of the other two groups comprised 4 mice. In the beginning, group C was injected with uscharidin into the abdominal cavity twice a week for 14 weeks, and the dose was calculated according to mouse body weight $2.0 \times 10^4 \mu\text{l}/\text{kg}$ each time.^[5,6] After hepatocarcinoma pattern had been set up on the 2nd, 4th, 6th, 8th, 10th, 12th, 14th, 16th, 18th, 20th, 22nd, and 24th week, one subgroup of all the 3 groups was killed to get two pieces of tissue in $1 \times 1 \times 1 \text{ cm}^3$ from the right and the left liver for microscopic observation.

Counting of tumor nodes

The sections were placed under a microscope to count cancer nodes and under a grid ocular scape to measure whether the area of nodes was greater than 0.05 mm^2 , which represents the general situation of hepatocarcinoma.

RNA extraction

Initially the preserved liver tissue (50-100 mg) was mixed and grinded evenly with 1 ml of cold denaturant. One ml lysis liquid was put into a 2.0 ml centrifuging tube and then mixed with 0.1 ml of 2 mol/L sodium acetate (pH 4.0). The liquid was further mixed with 1 ml phenol/chloroform mixture and vibrated for 10 seconds and then put on ice for 10 minutes. Refrigerated centrifugation was kept under 4 °C and the liquid in the tube was in three layers including red phenol/chloro-

form at the bottom, white protein in the middle, and water-like liquid in the top (RNA). The top layer liquid was transferred into a 1.5 ml centrifuging tube and kept below -20 °C for 15 minutes after mixing with isopropanol of identical volume. White jelly-like precipitate observed after centrifugation at 10 000 g for 15 minutes under 4 °C was found to be total RNA. RNA was dissolved completely by 1 ml of denaturant. The above procedures were to purify RNA, RNA precipitate and the wall of the tube were washed, and RNA was dissolved in Rnase-free water and preserved below -20 °C.

RNA assessment

The optical density (OD) value of the preserved total RNA was measured by an ultraviolet spectrophotometer and the RNA concentration was calculated by the equation of $(\text{OD}_{260} \times \text{nucleic acid dilution times} \times 40/1000) / (\text{OD}_{260}/\text{OD}_{280}) > 1.8$. If the OD of RNA was greater than 1.8, the RNA was pure enough to be used in the following experiment.

Agarose electrophoresis

Dispensed 2% sepharose containing a small quantity ethidium bromide (EB), 1 μl of RNA, and 2 μl of bromphenol blue buffer were mixed subsequently Exponent was added rapidly and electrophorated in an electrophoresis chamber treated Rnase-free at 100 V for 20 minutes. After electrophoresis, the gelatum was observed under a burdick lamp. If the RNA purity and the condition of electrophoresis were suitable, three RNA straps of 28 seconds, 18 seconds, 5 seconds would be seen through the device of gel electrophoresis.

DNA synthesis

Total RNA (2 μl or 1 μg), c-myc primer (4 μl or 20 pmol), and RNA-free (8 μl) were mixed well at the room temperature. Then the mixture was degenerated in water bath at 70 °C for 5 minutes, put on ice for 1 minute, and centrifugated at 200 g for 30 seconds. M-MLV 5 \times buffer (5 μl), dNTP (5 μl or 2.5 mmol/L), rRNA (5 μl or 20 μg), and M-MLV RT (5 μl) were added into the mixture, with a total response volume of 34 μl . After mixing, the reverse transcriptase was inactivated at 42 °C for 60 minutes and at 95 °C for 5 minutes, and then it was kept at -30 °C.

PCR reaction

cDNA (16 μl), 10 \times buffer (no MgCl_2) (5 μl), MgCl_2 (3 μl or 25 mmol/L), dNTP (4 μl or 2.5 mmol/L), sense (3 μl or 15 pmol), antisense (3 μl or 15 pmol), Taq enzyme (1 μl or 3 μl), and RNA-free water (9 μl) were mixed at the room temperature with a total response volume of 50 μl . The mixture was put in a PCR cycle after a drop of paraffin oil treated by high temperature was added and degenerated at 94 °C for

5 minutes at 94 °C, 50 °C and 72 °C respectively. Each temperature was kept for 1 minute, lasted 35 times, and extended finally at 72 °C for 5 minutes.

In agarose electrophoresis, c-myc DNA product (8 μ l) was taken to undertake caraphoresis with 2% sepharose containing a small quantity of EB and two straps, 228bp and 120bp, were found under the burdick lamp. Gel image pattern analysis system of OD scanned the caraphoresis strap of PCR and quantitative reaction, while forming the image of gel electrophoresis and keeping the image in computer.

Statistical analysis

The results were analyzed by software SPSS11. The chi-square test was used to compare the incidence rate of cancer and the area of cancerous nodes in the cancer induction and intervention groups at different time. A *P* value less than 0.05 was considered significant. The c-myc mRNA inter-group was analyzed with single factor analysis of variance and LSD method, showing that a *P* value less than 0.05 was significantly different.

Results

Pathomorphological changes of mouse liver in group B

In group B, pathological changes could be classified into early, middle and late stages. In the early stage from the 1st week to the 8th week, the shape of the liver was slightly enlarged. In the middle stage from the 9th week to the 14th week, the liver was swollen and brown. From the 12th week, the number of lesions increased gradually and the liver turned to be hard. From the 14th week onward, liver cirrhosis occurred. In the late stage from the 16th week to the 24th week, nodosity augmented the size of the liver, and the edge of the liver could reach the pelvic cavity. Under a light microscope, from the 2nd week, cell proliferation was seen in the portal area, and gradually, a large amount of cells proliferated and migrated into the liver parenchyma (Fig. 1). From the 10th to the 14th week, lots of multiformed pseudolobules of proliferated fiber tissue appeared in the liver parenchyma, and the lobules' cells varied in

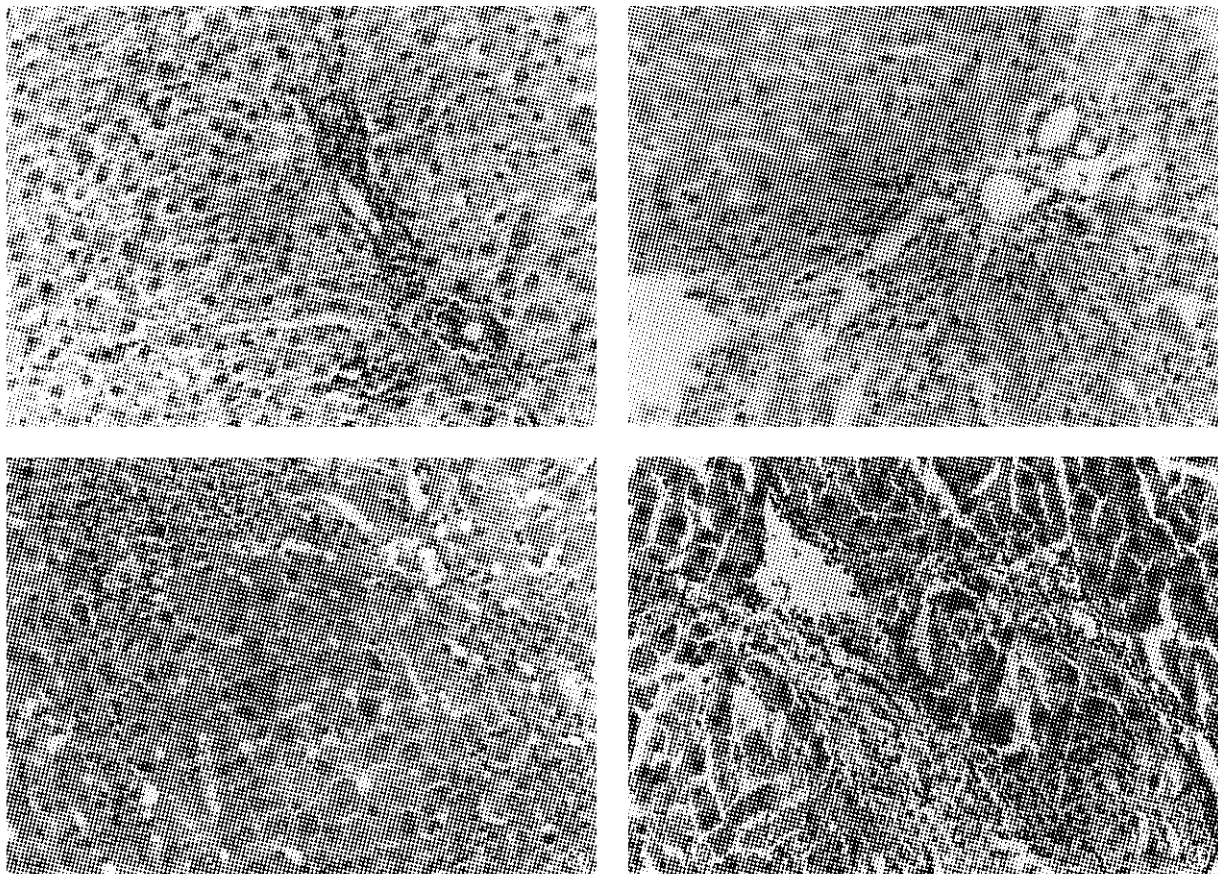


Fig. 1. Oval cells at the portal area at the early stage of inflammatory change in group B at the 2nd week.

Fig. 2. A lot of multiformed pseudolobules of fiber tissue proliferated in the liver parenchyma. The liver cells were of atypical hyperplasia, and oval cells gathered around the portal area in group B at the 12th week (HE, original magnification $\times 200$).

Fig. 3. A lot of oval cells gathered around cancer nodes in group B at the 20th week (HE, original magnification $\times 200$).

Fig. 4. Mixed pattern of cancer tissue in group B at 24th week (HE, original magnification $\times 200$).

Table 1. Number of cancer nodes and cancer nodes area in groups B and C (mean±SD, n=8)

Time (wk)	Hepatic cancer		Cancer nodes		Cancer node area (mm ²)	
	Group B	Group C	Group B	Group C	Group B	Group C
2-4	0	0	0	0	0	0
6-8	0	0	0	0	0	0
10-12	2	0	4	0	9.5±8.2	0
14-16	6	2	15	5	10.7±8.7	5.8±4.5 [#]
18-20	8	4	17	9	11.4±8.9	8.5±7.6
22-24	8	4	16	10	11.2±9.3	8.6±7.3

#: *P*<0.05 vs. group B. Group B; induction group; group C; intervention group.

size. Numerous oval cells proliferated in the portal area, and migrated into lobules and nodes (Fig. 2). From the 16th to the 24th week, cancer cell nuclei sized differently and karyokinesis happened often. Cancer cells infiltrated toward the periphery of liver tissue and oval cells could be seen in cancer nodes (Figs. 3 and 4). In the fibrosis period of liver proliferation, piles of oval cells proliferated in both the portal area and its peripheral area. The volume of oval cells was one third of normal liver cells. Oval cells were round or oval in shape, with cytoplasm, basophilia, and unclear margin. The nucleus was round or oval, lightly colored with clear membrane but obvious nucleolus.

Uscharidin's effect on cancer induction

In group C, from the 2nd week to the 8th week the liver of mouse appeared normal and slightly hypere-

Table 2. C-myc relative gray value

Time (wk)	Group A (n=4)	Group B (n=8)	Group C (n=8)
2-4	1.02±0.31	1.27±0.95 ^a	1.17±0.58 ^a
6-8	1.05±0.41	2.03±0.64 ^a	1.52±0.71 ^{a*}
10-12	1.10±0.54	3.56±1.21 ^b	2.23±0.87 ^{a*}
14-16	1.29±0.36	5.69±1.35 ^b	3.53±0.92 ^{b*}
18-20	1.27±0.63	7.83±1.44 ^b	6.54±1.09 ^{b*}
22-24	1.34±0.43	8.16±2.18 ^c	8.01±1.26 ^{c*}

*: compared with group B, *P*>0.05; a: compared with group A (normal group), *P*>0.05; b: compared with group A, *P*<0.05; c: compared with group A, *P*<0.01.

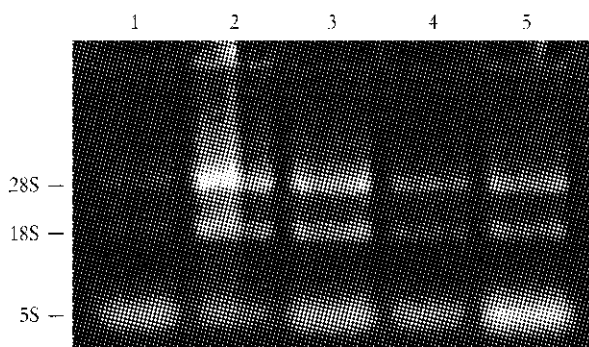


Fig. 5. Electrophorogram of the total RNA of the rat liver tissue.

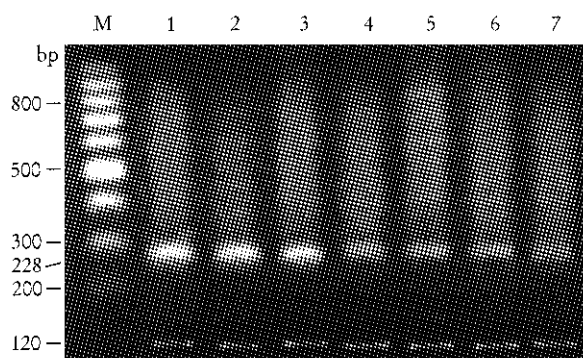


Fig. 6. C-myc mRNA expression levels in the rat liver tissue detected by RT-PCR. The upper cord of 228bp was c-myc and the lower cord of 120bp was β-actin. Lanes 1 and 2; tissue of hepatocarcinoma; Lane 3; tissue of cirrhotic liver; Lanes 4, 5 and 6; tissue of inflammatory change; and Lane 7; normal tissue.

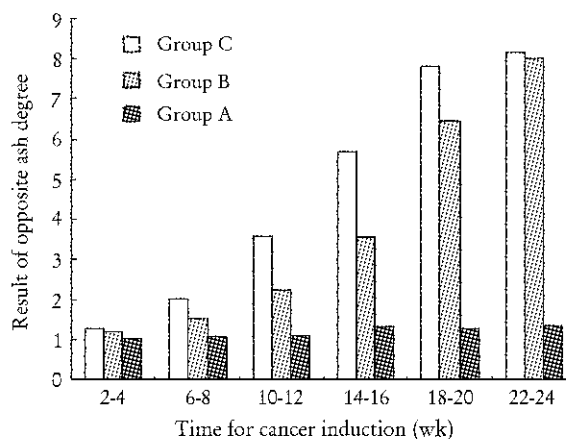


Fig. 7. Change of c-myc mRNA in cancer induction.

mic. In the period of the 10th-14th week, the mouse liver was swollen with grey color. Edematous degeneration of liver cells was obvious with local necrosis of cells, proliferation of fiber, and pseudobubulation. In the period of the 16th-24th week, the liver further swollen to a diameter of 0.2 cm, with nodes and oval cells in the plexus of cancer cells. The member of tumor nodes is shown in Table 1, and c-myc relative gray value in Table 2, Figs. 5-7).

The data on relative expression of c-myc mRNA in the hepatic tissues of mice of different groups in the different stages of carcinoma are shown in Table 2, Figs. 5 and 6. C-myc relative gray value indicated the proportionality of c-myc gray value to β -actin gray value.

Discussion

Pathological changes of oval cells during hepatocarcinogenesis

Oval cell was round or oval with little cytoplasm and basophilia, and its nucleus was round or oval, with light color and clear membrane but its nucleolus was small and clear. When liver cell was strongly injured or its proliferation was inhibited, oval cell differentiated toward liver cell and bile duct epithelial cell,^[7,8] so it is a kind of ancestral cell with a potential of bi-directional differentiation. In this study, at the 2nd week after the liver was attacked by DAB, oval cells were noted on the epithelial layer of the bile duct. As the liver was further infected by virus, the cells proliferated gradually and gathered in the portal area. At the same time, it immigrated into the liver parenchyma. At the 4th week after the liver was involved with DAB, oval cells were seen in part of the liver parenchyma close to the portal area. Pathomorphological changes in liver tissue at different time showed that oval cell was associated with hepatocarcinogenesis. At the peak of proliferative fibrosis, oval cells were seen in all the field of vision, and they piled up like a ball in the area of fibrous proliferation. Moreover oval cells could be seen in pseudolobules. During canceration, a large number of oval cells gathered around cancer nodes or inside the nodes. Hence, we consider that oval cells play an important role in hepatocarcinogenesis. Oval cells originate from the bile duct epithelia in the portal area, and as soon as the liver is damaged, fibrous proliferation may be increased gradually to injury the liver parenchyma. The more liver fiber sediments, the more oval cells collect; but the mechanism making oval cell to emigrate into liver fiber is not clear. We think that it may be related to a large amount of factors such as IL-1, IL-6, TNF- α , which are given off by liver tissue when the liver is damaged. The arrival of inflammatory factors in the liver tissue could activate Ito cells^[9,10] in the spaces between liver sinusoids. The activated Ito cell could change into myofibroblaster (MFB) through its superficial type, and produce intercellular adhesion molecule-1 (ICAM-1) to boost liver fibrosis.^[11-15] ICAM-1 could attract lymph cells to the area of Ito cell proliferation for strengthening inflammatory reaction. In addition, in the cell regeneration of residual liver tissue after partial removal of the liver, liver cells take 15 hours entering period of DNA synthesis after the G₀ period. The earliest cell entering the cell circle is Ito cell, then oval cell is activated.^[16] This indicates that the activation of

Ito cell is the premise of that of oval cell.

Expression of c-myc mRNA in mouse with hepatocarcinoma

C-myc is a maintaining gene for malignant tissue and its gene code protein is DNA conjugated protein with the function of transcription regulation in the nucleus.^[17-19] Increased expression of c-myc could be observed in both hepatocarcinoma tissue and para-hepatocarcinoma tissue. The effect of c-myc on the development of hepatocarcinoma was controversial^[20-22] that increased expression of c-myc is one of the factors causing hepatocarcinoma, and that in the late stage of hepatocarcinoma it is merely a characteristic of the stage and an indication of continuous proliferation of cells. Experiment^[23,24] has proved that c-myc expression has nothing to do with cell proliferation, but is related to the integration of virus. The increased expression of c-myc is slightly correlated with the appearance of hepatic injury and progressively with the severity of hepatic injury. In the course of canceration, the expression of c-myc mRNA also tends to increase with the development of hepatocarcinoma. c-myc as a carcinogene might be a promoter gene for hepatocarcinoma, the presence of c-myc significantly affects the maintainance of hepatic injury and carcinomatous change of hepatocytes. During the development of carcinoma, the expression of c-myc continues to increase, indicating that c-myc is not only a maintaining gene for malignant carcinoma, but its expression level is a symbol gene for the degree of malignancy and development of hepatocellular carcinoma. The development of hepatocellular carcinoma is closely related to oval cell, but is the expression of c-myc related to oval cell? Reports^[25,26] suggested that the overexpression of c-myc in the proliferated cell-focus and the expression of oncogene rarely in hepatocytes around the cell-focus could be seen after in situ hybridization. Identified cell types of the proliferated cell-focus showed that oval cell is predominant and c-myc is a dominantly expressed oncogene.^[27,28] It is shown that hepatic stem cells, represented by oval cells are closely related to the onset and development of hepatocellular carcinoma in terms of cells, protein or gene.

Uscharidin's effect on mouse hepatocarcinoma

Uscharidin is a kind of broad-spectrum trypsin inhibitor abstracted from the urine of human beings and its end product is a kind of white powder, which can be dissolved in water or saline. Uscharidin can be used for intravenous drip or abdominal injection to inhibit the secretion of trypsin, wydase, elastase, and chymotrypsin. But part of degradation products remains to be of enzyme-inhibition competence. Uscharidin is obviously effective in anti-shock and anti-inflammation, protection of renal function, minimization of damage to the

related organs before and after operation, and prevention of cancer cell metastasis.^[29] Researchers reported the combination site with uscharidin on the surfaces of all kinds of tumor cell membrane, and uscharidin inhibits via its combination with the recipient on the surface of tumor cell membrane, the secretion of protein lyase, fibrinoclastase, matrix metalloproteinase and collagenase of tumor cell competently secreting granulocytes.^[30] These enzymes could degrade the peripheral matrix and boost tumor cells to metastasis. Other report showed that uscharidin was combined with other anti-cancer drugs to inhibit the metastasis of tumor cells.^[31] It is true that clinical urinary trypsin inhibitor is obviously effective in cancer control. In this experiment, uscharidin was involved the incidence of hepatocarcinoma so as to observe its influence on hepatocarcinoma pattern-setting. The incidence of hepatocarcinoma in group C was lower than that in group C ($P < 0.05$). In conclusion, the incidence of hepatocarcinoma needs a micro-environment. Uscharidin may inhibit some cells to release inflammatory medium by stabilizing lysosome membrane and clear away oxygen-derived free radicals on the surfaces of liver cells and oval cells, thus preventing liver tissues from being damaged.

Uscharidin can inhibit the development of hepatic injury and hepatocellular carcinoma to some extent, but can not inhibit the expression of c-myc. The expression of c-myc is closely related to the degree of hepatic injury.

Competing interest

No benefits in any form have been received or will be received from a commercial party related directly or indirectly to the subject of this article.

References

- Paku S, Schnur J, Nagy P, Thorgeirsson SS. Origin and structural evolution of the early proliferating oval cell in rat liver. *Am J Pathol* 2001;158:1313-1323.
- Faris RA, Konkin T, Halpert G. Liver stem cell: a potential source of hepatocyte for the treatment of human liver disease. *Artif Organs* 2001;25:513-521.
- Mao H, Zhao MF, Feng JJ. The change of IL-2, malonyl dialdehyde in rats induce liver carcinoma by DAB. *Chin J Gastroenterol* 1999;8:175-176.
- Zhang JZ. Carcinohistogenesis and expression of alpha fetoprotein in experimental hepatocarcinoma. *J Clin Exp Pathol* 1999;15:224-226.
- Okuhama Y, Shirashi M, Higa T, Tomori H, Taira K, Mamadi T, et al. Protective effects of ulinastatin against ischemia-reperfusion injury. *J Surg Res* 1999;82:34-42.
- Koizumi R, Kanai H, Maetzawa A, Kanda T, Nojima Y, Naruse T. Therapeutic effects of ulinastatin on experimental crescentic glomerulonephritis in rats. *Nephron* 2000;84:347-353.
- Thorgeirsson SS. Hepatic stem cells in liver regeneration. *Faseb J* 1996;10:1249-1256.
- Badve S, Logdberg L, Sokhi R, Sigal SH, Botros N, Chae S, et al. An antigen reacting with das-1 monoclonal antibody is ontogenically regulated in diverse organs including liver and indicates sharing of developmental mechanisms among cell lineages. *Pathobiology* 2000;68:76-86.
- Benedetti A, Di-Sario A, Casini A, Ridolfi F, Bendia E, Pignini P, et al. Inhibition of the NA(+)/H(+) exchanger reduces rat hepatic stellate cell activity and liver fibrosis: an in vitro and in vivo study. *Gastroenterology* 2001;120:545-556.
- Toda K, Kumagai N, Tsuchimoto K, Inagaki H, Suzuki T, Oishi T, et al. Induction of hepatic stellate cell proliferation by LPS-stimulated peripheral blood mononuclear cells from patients with liver cirrhosis. *J Gastroenterol* 2000;35:214-220.
- Xu J, Geng ZM, Ma QY. Microstructural and ultrastructural changes in the healing process of bile duct trauma. *Hepatobiliary Pancreat Dis Int* 2003;2:295-299.
- Gong JQ, Fang CH, Li Y, Tian FZ. The experimental study on the oval cells participating in hepatocarcinogenesis. *Zhonghua Wai Ke Za Zhi* 2004;42:291-295.
- Fang CH, Zhang W, Zhu XY, Gong JQ, Zhang GQ. The expression of c-kit and proliferating cell nuclear antigen in oval cells of rats with hepatocellular carcinoma. *Hepatobiliary Pancreat Dis Int* 2003;2:537-544.
- McCrudden R, Iredale JP. Liver fibrosis, the hepatic stellate cell and tissue inhibitors of metalloproteinases. *Histol Histopathol* 2000;15:1159-1168.
- Satoh T, Ichida T, Matsuda Y, Sugiyama M, Yonekura K, Ishikawa T, et al. Interaction between hyaluronan and CD44 in the development of dimethylnitrosamine-induced liver cirrhosis. *J Gastroenterol Hepatol* 2000;15:402-411.
- Gerlach C, Sakkab DY, Scholzen T, Dassler R, Alison MR, Gerdes J. Ki-67 expression during rat liver regeneration after partial hepatectomy. *Hepatology* 1997;26:578-578.
- Jonas JC, Laybutt DR, Steil GM, Trivedi N, Pertusa JG, van de Casteele M, et al. High glucose stimulates early response gene c-Myc expression in rat pancreatic beta cells. *J Biol Chem* 2001;276:35375-35381.
- Deng CX, Brodie SG. Roles of BRCA1 and its interacting proteins. *Bioessays* 2000;22:728-737.
- Fields WR, Desiderio JG, Putnam KP, Bombick DW, Doolittle DJ. Quantification of changes in c-myc mRNA levels in normal human bronchial epithelial (NHBE) and lung adenocarcinoma (A549) cells following chemical treatment. *Toxicol Sci* 2001;63:107-114.
- Satoh Y, Matsumura I, Tanaka H, Ezoe S, Sugahara H, Mizuki M, et al. Roles for c-Myc in self-renewal of hematopoietic stem cells. *J Biol Chem* 2004;279:1-32.
- Liu YC, Chen CJ, Wu HS, Chan DC, Yu JC, Yang AH, et al. Telomerase and c-myc expression in hepatocellular carcinomas. *Eur J Surg Oncol* 2004;30:384-390.
- Prochownik EV. c-Myc as a therapeutic target in cancer. *Expert Rev Anticancer Ther*. 2004;4:289-302.
- Chen CJ, Kyo S, Liu YC, Cheng YL, Hsieh CB, Chan DC, et al. Modulation of human telomerase reverse transcriptase in hepatocellular carcinoma. *World J Gastroenterol* 2004;10:638-642.
- Yamate J, Yasui H, Benn SJ, Tsukamoto Y, Kuwamura M, Kumagai D, et al. Characterization of newly established tumor lines from a spontaneous malignant schwannoma in F344 rats: nerve growth factor production, growth inhibition by transforming growth factor-beta1, and macrophage-like phenotype expression. *Acta Neuropathol (Berl)* 2003;106:221-233.

- 25 Nagy P, Everts RP, Marsden, Roach J, Thorgeirsson SS. Cellular distribution of c-myc transcripts during chemical hepatocarcinogenesis. *Cancer Res* 1988;48:5522-5527.
- 26 Galand P, Jacobovitz D, Alexandre K. Immunohistochemical detection of c-Ha-ras oncogene p21 product in pre-neoplastic and neoplastic lesions during hepatocarcinogenesis in rat. *Int Cancer* 1998;41:155-161.
- 27 Koster MI, Huntzinger KA, Roop DR. Epidermal differentiation: transgenic/knockout mouse models reveal genes involved in stem cell fate decisions and commitment to differentiation. *J Invest Dermatol Symp Proc* 2002;7:41-45.
- 28 Baudino TA, McKay C, Pendeville-Samain H, Nilsson JA, Maclean KH, White EL, et al. c-Myc is essential for vasculogenesis and angiogenesis during development and tumor progression. *Genes Dev* 2002;16:2530-2543.
- 29 Watt FM. The stem cell compartment in human interfollicular epidermis. *J Dermatol Sci* 2002;28:173-180.
- 30 Kobayashi H, Gotoh J, Fujie M, Terao T. Characterization of the cellular binding site for the urinary trypsin inhibitor. *J Biol Chem* 1994;269:20642-20647.
- 31 Kobayashi H, Shinohara H, Gotoh J, Fujie M, Fujishiro S, Terao T. Anti-metastatic therapy by urinary trypsin inhibitor in combination with an anti-cancer agent. *Br J Cancer* 1995;72:1131-1137.

Received December 26, 2003

Accepted after revision March 20, 2004

Now go, write it before them in a table, and note it in a book.

— Isaiah 30:8